analytical chemistry

Article

Cite This: Anal. Chem. 2018, 90, 1142−1146

pubs.acs.org/ac

Ultrasensitive Electroanalysis: Femtomolar Determination of Lead, Cobalt, and Nickel

Min Zhou,[†,‡] Jeffrey E. Dick,[†,‡] Keke Hu,[§] Michael V. Mirkin,[§] and Allen J. Bard*[,†]

[†]Center for Electrochemistry, Department of Chemistry, The University of Texas at Austin, Austin, Texas 78712, United States

[§]Department of Chemistry and Biochemistry, Queens College, City University of New York, Flushing, New York 11367, United States

Supporting Information

ABSTRACT: We demonstrate the feasibility of attaining femtomolar limits of quantitation in electroanalysis. The method employed is based on electrocatalytic amplification, where small quantities of metal deposit performed on a carbon electrode causes a large increase in the observed current, for example, for the oxidation of water. We show calibration curves at the femtomolar level for cobalt, nickel, and lead ions on carbon ultramicroelectrodes (CUMEs), ca. 500 nm radii. The CUME was biased at a potential where the ion would deposit as the metal oxide, MOx, and a high concentration of species that is oxidized at the deposit is present in solution. Blips were observed in the amperometric *i*−*t* response, and their frequency scaled linearly with the concentration of ions at the femtomolar level. From these results, the limits of quantitation for cobalt, nickel, and lead ions were reported at 10 s of femtomolar level for the first time.

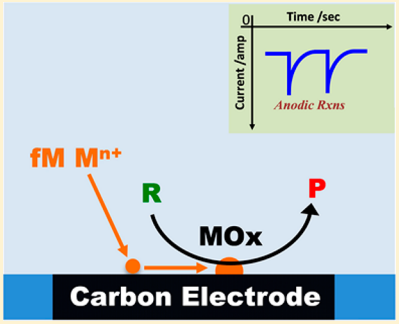

Sensitive electroanalytical techniques for the determination of metals have been developed. Perhaps the technique with the lowest limit of detection (LOD) is stripping analysis. In this case a bulk electrolysis to deposit the metal in a mercury drop or other small electrode is carried out and the contents determined from a linear scan voltammogram. The LOD is typically at the nanomolar level. Reported here is a method orders of magnitude more sensitive. Analytical chemistry is entering a digital era where, instead of measuring ensemble amounts of large numbers of analyte atoms or molecules, analyte species can be detected and counted one at a time.[1] Inherent in these experiments are LODs of a single analyte, for example, nanoparticle (NP) or molecule and limits of quantitation of solution concentrations that are subpicomolar.[2,3] Over the past decade, stochastic electrochemical processes have been explored and extended to a variety of NPs.[4−11] In these experiments, picomolar or lower concentrations are used to ensure one particle moves to the electrode every few seconds. For instance, one method for detecting catalytic nanoparticles is electrocatalytic amplification, which was developed by our group in 2007.[12] These experiments are based on the principle that some heterogeneous reactions are faster on some materials than others. For example, proton reduction is faster on platinum than on carbon. Observations indicate that if a carbon fiber electrode is biased at a potential where proton reduction occurs on platinum but not carbon in an acidic solution, the faradaic response of single platinum nanoparticles (Pt NPs) can be observed when colliding with the carbon surface.

Conceptually, at an ionic level, $PtCl_6^{2-}$ will reduce to Pt^0 on a carbon electrode at a potential where proton reduction can occur on the electrodeposited platinum species.[13] The concentration of $PtCl_6^{2-}$ was held at the femtomolar level so that one ion would diffuse to and interact with the electrode surface every few seconds. Blips were observed in the amperometric *i*−*t* response, which showed to be indicative of hydrogen evolution catalysts.[13] Studying the mechanism of the deposition, the blips in the amperometric response scaled linearly with the concentration of $PtCl_6^{2-}$. This linear relationship constitutes a calibration curve for femtomolar levels of $PtCl_6^{2-}$, which is one of the lowest limits of quantitation in modern analysis. While continuing to probe the mechanism of the electrodeposition and electrocatalysis mechanisms on these deposits, we aim to demonstrate the ultrasensitivity of this electroanalytical method for other metal ions in this communication.

In particular, we demonstrate here the feasibility of attaining calibration curves for cobalt, nickel, and lead at the femtomolar level. In experiments with cobalt or nickel, phosphate buffered solution (PBS) was used. Cobalt or nickel oxide with phosphate has been shown to be a good water oxidation catalyst and can oxidize water when deposited on a carbon electrode.[14] When the electrode was biased sufficiently positive such that cobalt or nickel oxide would electrodeposit and catalyze water oxidation, blips were observed in the amperometric response. Likewise, PbO_2 has been shown to oxidize methanol to CO_2. When the potential of the electrode was held positive in a methanol solution for Pb^{2+} to deposit, blips were observed in the

Received: August 18, 2017
Accepted: December 7, 2017
Published: December 7, 2017

DOI: 10.1021/acs.analchem.7b03355
Anal. Chem. 2018, 90, 1142−1146

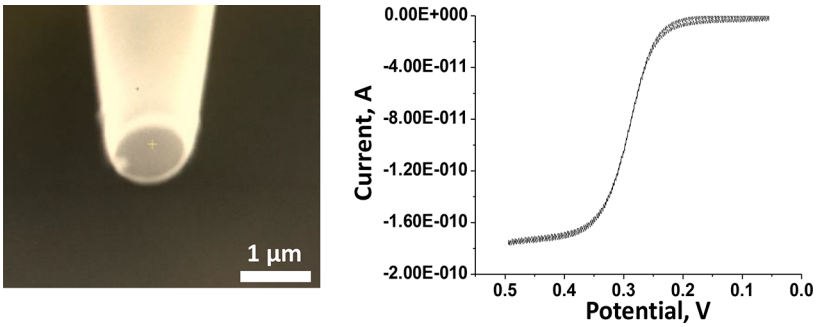

Figure 1. SEM image and cyclic voltammogram of a typical FIB milled carbon nanopipette (radius, 510 nm). The used solution was 1 mM FcMeOH and 0.2 M KCl. Scan rate was 50 mV/s.

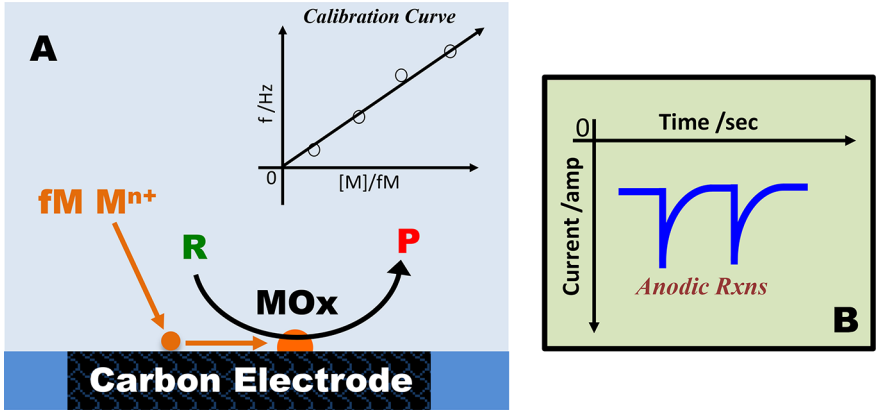

Figure 2. (A) Schematic representation of anodic deposition experiment to drive a reaction where reactants (R) are converted to products (P). Inset of (A) shows the calibration curve between the spike frequency and the ion concentration. (B) Schematic of the amperometric response for anodic reaction.

amperometric *i*–*t* trace. In each of the cases mentioned above, the frequency of blips scaled linearly with the concentration of ions at the femtomolar level.

EXPERIMENTAL SECTION

Chemicals and Materials. Cobalt nitrate (98%), nickel nitrate (98%), lead acetate (97%), and anhydrous methanol were purchased from Sigma-Aldrich and used as received. Ferrocenemethanol (FcMeOH, 97%) was purchased from Alfa Aesar. Water used during the experiments was Milli-Q (18.3 MΩ/cm, EDM Millipore, MA, TOC < 3 ppb). Solutions prepared for electrochemical measurements were prepared and then filtered with a 0.1 μm diameter pore (Millex-Syringe, PVDF 0.1 μm, Merck Milliipore Ltd.). The 1.0 M phosphate buffer solution at pH 8.0 was prepared by mixing certain molar ratio of K_2HPO_4 and KH_2PO_4. The 10s and 100s of femtomolar metal ion solutions were prepared based on a previously reported procedure.[13,14] All the used chemicals and materials were indicative of high purity, and the containers and electrochemical cell were carefully soaked in piranha solution and then sonicated in 10% nitric acid to remove organic and inorganic impurities. For the measure of lead ions, to avoid lead contamination from air, we carefully prepared the solutions in the chamber, stored them in closed precleaned containers, and measured in an airtight electrochemical cell.

Carbon Ultramicroelectrode (CUME) Fabrication and Characterization. Two different CUMEs were used in this study. Carbon fiber microelectrodes were fabricated by sealing a carbon fiber in a glass capillary. Electrical contact was made to the carbon fiber by silver epoxy. The sealed capillary was mechanically polished until the surface of the carbon fiber was exposed.[13]

The pyrolyzed methane CUME was fabricated as follows.[15] A cone-shaped nanopipette was pulled from a quartz capillary (O.D.1.0 mm and I.D. 0.7 mm, Sutter Instrument, Novato, CA) and deposited with carbon by chemical vapor deposition. A nanopipette with a tip diameter from 10 to 100 nm was fabricated by using a CO_2 laser puller (P-2000, Sutter Instrument) based on a program of HEAT = 800, FIL = 4, VEL = 22, DEL = 128, PUL = 110, and HEAT = 830, FIL = 3, VEL = 17, DEL = 130, PUL = 255. The nanopipette was nearly completely deposited and filled with pyrolysis of carbon using methane as the carbon source and argon as the protector for 1 h at 900 °C. We used a copper nickel wire (0.13 mm diameter, Alfa Aesar, Ward Hill, PA) to establish a connection with a carbon nanopipette for electrochemical measurements as well as its grounding to a sample stage in SEM, and FIB experiments, and for protection from electrostatic damage. A carbon nanopipette with a desirable radius was milled by using an FIB instrument to yield a flat carbon UME. A typical FIB milled carbon nanopipette and electrochemical oxidation of 1 mm FcMeOH in 0.2 M KCl on it are given in Figure 1.

Electrochemical Measurements. All the experiments were carried out with a CHI 900C potentiostat. The working electrode was FIB milled carbon nanopipette with a typical radius of about 500 nm. The reference electrode was Ag/AgCl/1.0 M KCl. The counterelectrode was a large graphite rod. In ion collisions, the sampling rate of the amperometric *i*–*t* curve was 50 ms that is useful in achieving a high signal/noise ratio. The filtering frequency used the default setup. The cell-on

DOI: 10.1021/acs.analchem.7b03355
Anal. Chem. 2018, 90, 1142–1146

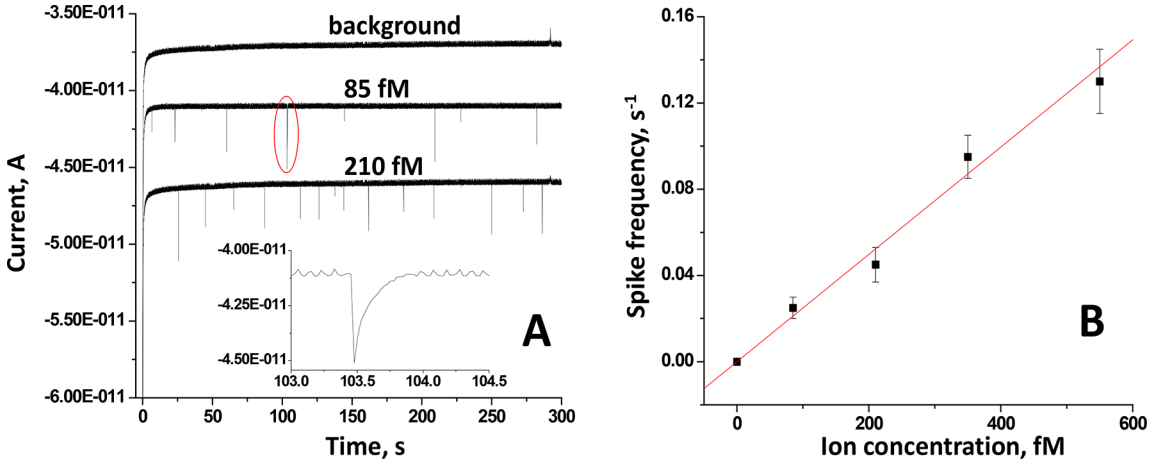

Figure 3. (A) Amperograms of carbon nanoelectrode (radius, 510 nm) poised at 1.2 V in the blank 1.0 M PBS, pH = 8.0 and cobalt(II) ions containing solutions, where $Co(NO_3)_2$ concentrations were, respectively, 85 and 210 fM. Other experimental conditions can be found in the Experimental Section. Inset shows the red marked transient. The *i*−*t* curves were offset for clarity, except for the background recording. (B) Linear relationship between the observed transient frequency and the cobalt(II) ion concentration. The goodness of the linear fit is R^2 = 0.97.

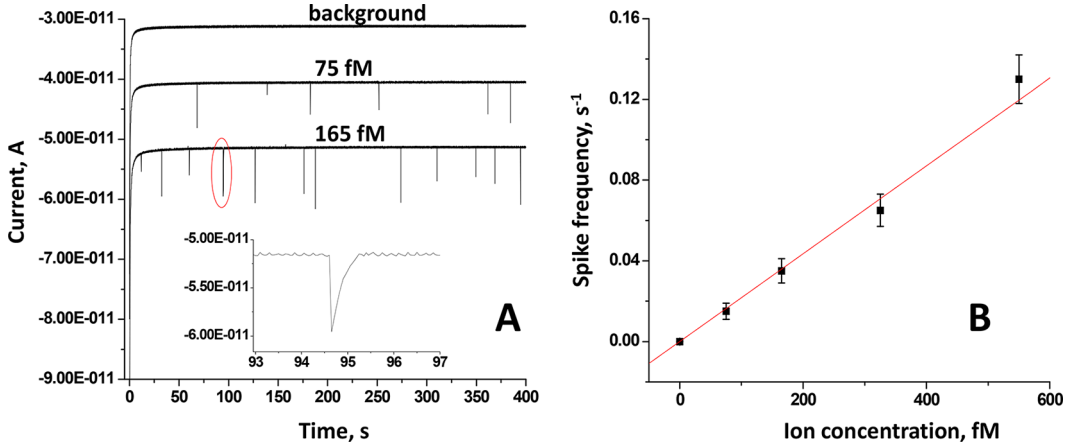

Figure 4. (A) Amperograms of carbon nanoelectrode (radius, 545 nm) biased at 1.25 V in the blank 1.0 M PBS, pH = 8.0 and nickel(II) ions containing solutions, where $Ni(NO_3)_2$ concentrations were, respectively, 75 and 165 fM. Other experimental conditions can be found in the Experimental Section. Inset shows the red marked transient. The *i*−*t* curves were offset for clarity except for the background recording. (B) Linear relationship between the observed transient frequency and the used nickel(II) ion concentration. The goodness of the linear fit is R^2 = 0.98.

function in potentiostat was switched on during electrochemical measurements, which were useful to protect the CUME and its deposit. In addition, the electrostatics damage protection (i.e., connecting the operator and the samples with the real ground) was rigorously adopted to shield CUME and its deposit. All related sensitive electrochemical measurements were conducted in a well-grounded Faraday cage to remove any outside noise. The electrochemical cell was a homemade Teflon container with a maximum volume of 5 mL. The Teflon material shows very weak adsorption of the detected metal ions. The experiments of cobalt and nickel ions were conducted in aqueous solutions, and different from them, the analysis of lead, which ions was carried out in a pure methanol solvent. For counting the observed frequency, the spikes were selected based on shape and relative amplitude compared to the background current. The spike shape of the analytical transients were asymmetric *i*−*t* trace (fast rise and exponential decay) of rather long duration, for example, 200 ms, while background ones were symmetrical and sharp (limited by sampling rate). Sample transients were typically at least 5× the background level.

RESULTS AND DISCUSSION

Figure 2A shows a generalized schematic representation of the deposition experiments. A metal precursor ion is initially dissolved in a solvent at femtomolar levels. In these experiments, the diffusion of ions to the electrode surface is stochastic. When the ions are deposited on the electrode surface at a potential, where the reaction, R → P, proceeds, blips in the amperometric *i*−*t* response (Figure 2B) were observed. Cobalt and nickel follow the general experimental setup for electrocatalytic amplification experiments as previously reported by our group as a means of observing catalytic nanoparticle collisions on UMEs.[13,14] For example, the deposition for cobalt or nickel was carried out in PBS, and the potential was held sufficiently positive for cobalt(III) or Ni(III) oxide to form. The potential was also sufficiently positive for the oxide to catalyze water oxidation. The lead detection followed a slightly different reaction pathway (vide infra). The stochastic flux of ions to the electrode surface can be modeled by the average frequency (f) with which ions interact with the electrode under diffusion control, given by eq 1 below:

DOI: 10.1021/acs.analchem.7b03355
Anal. Chem. 2018, 90, 1142−1146

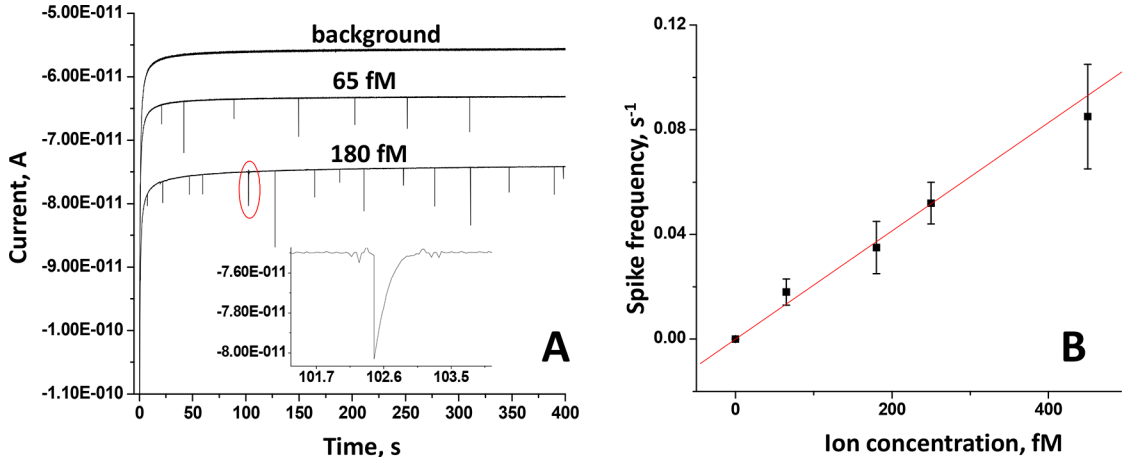

Figure 5. (A) Amperograms of carbon nanoelectrode (radius, 520 nm) poised at 1.5 V in the blank 0.1 M $TBAPF_6$ and lead(II) ions containing methanol solutions, where Pb(Ac)2 concentrations were, respectively, 65 and 180 fM. Other experimental conditions can be found in the Experimental Section. Inset shows the red marked transient. The $i-t$ curves were offset for clarity except for the background recording. (B) Linear relationship between the observed transient frequency and the used lead(II) ion concentration. The goodness of the linear fit is $R^2 = 0.99$.

$$f = 4.64 D_{ion} c_{ion} a N_A \quad (1)$$

where 4.64 factor responses to a limited RG (ca. 1.35) of CUME. RG is defined as the ratio between the insulator thickness and the radius of the electrode. D_{ion} is the diffusion coefficient of the metal ion (ca. 1.0×10^{-5} cm^2/s), C_{ion} is the concentration of the metal ion, a is the radius of the electrode, and N_A is Avogadro's number (6.02×10^{23} mol^{-1}). Thus, the concentration of ions required for one ion to interact with the electrode every 10 s ($f = 0.1$ Hz) for a carbon electrode with a = 500 nm and 5 μm is 75 and 7.5 fM, respectively.

Figure 3A gives the amperometric response for various concentrations of Co^{2+} (as $Co(NO_3)_2$) in 1.0 M PBS. The applied potential was 1.20 V versus Ag/AgCl with a graphite rod as the auxiliary electrode. All experiments were carried out on a pyrolyzed carbon nanoelectrode. Details of the nanoelectrode fabrication are given in the methods section. Figure 3B shows the calibration curve of cobalt at femtomolar levels. The average charge passed during the response was 0.75 ± 0.13 pC. The overall decrease in the background current is likely due to the oxidation of the carbon of the surface at the relatively high potential.

Figure 4A gives the amperometric response and calibration curve for various concentrations of Ni^{2+} in 1.0 M pH 8.0 PBS. The applied potential was 1.25 V versus Ag/AgCl. At this potential, nickel ions will deposit to Ni(III) oxide, and the metallic oxide deposit will catalyze the oxidation of water over the carbon background. For experiments with nickel, the average charge passed during the response was 2.25 ± 0.18 pC. Figure 4B shows the calibration curve obtained at this level.

Figure 5A gives the amperometric response for Pb^{2+} detection in methanol. We also show in the Supporting Information experimental results using a carbon fiber UME, which shows similar results to the nanoelectrodes. Figure 5B shows the frequency of blips as a function of lead concentration. The electrocatalytic amplification, reaction on PbO_2 involves the oxidation of a high concentration of methanol. Lead is deposited as PbO_2, which reacts with methanol to form Pb^{2+} and products of methanol oxidation on PbO_2.

$$Pb^{2+} + 2H_2O - 2e^- \rightarrow PbO_2 + 4H^+ \quad (2)$$

$$PbO_2 + MeOH \rightarrow Pb^{2+} + \text{products} \quad (3)$$

The Pb^{2+} that is regenerated during methanol oxidation is then redeposited as PbO_2. The average charge passed during the response was 1.36 ± 0.33 pC.

CONCLUSIONS

In this paper, we have sought to demonstrate the efficacy of obtaining calibration curves at the femtomolar level using micro- and nanoelectrodes. To the best of our knowledge, this technique is the most sensitive electroanalytical technique developed for the detection of ions under very dilute conditions. The requirement for these experiments is that a metal or metal oxide is formed that will catalyze the oxidation or reduction of a solution species in very high concentration. Thus, amplification is obtained by taking advantage of the difference in kinetics between the substrate electrode and the deposit. While the limits of quantitation imply that only a few number of atoms are responsible for the response, we are actively investigating the mechanism of nucleation and growth of the catalytic species in these dilute systems.

Note that improvements in sensitivity beyond what is demonstrated here is possible. For example, one can combine the stripping voltammetry strategy with analysis of the type shown here. Depending on the effectiveness of the bulk deposition process and the efficiency of the stripping, one should be able to obtain at least 2 orders of magnitude improvement in the LOD. One can also investigate substrate electrodes that are "anticatalytic" and showing lower background currents.

ASSOCIATED CONTENT

Supporting Information

The Supporting Information is available free of charge on the ACS Publications website at DOI: 10.1021/acs.analchem.7b03355.

Amperograms of lead(II) ion collisions on carbon fiber UME (PDF).

DOI: 10.1021/acs.analchem.7b03355
Anal. Chem. 2018, 90, 1142−1146

AUTHOR INFORMATION

Corresponding Author

*E-mail: ajbard@cm.utexas.edu. Phone: +1 5124713761.

ORCID

Jeffrey E. Dick: 0000-0002-4538-9705
Michael V. Mirkin: 0000-0002-3424-5810
Allen J. Bard: 0000-0002-8517-0230

Author Contributions

‡These authors contributed equally to this work.

Notes

The authors declare no competing financial interest.

ACKNOWLEDGMENTS

This work was supported by the National Science Foundation (CHE-1405248, AJB; DGE-1110007, JED; CHE-1300158, MVM) and the Welch Foundation (F-0021).

REFERENCES

(1) Kim, J.; Dick, J. E.; Bard, A. J. *Acc. Chem. Res.* **2016**, *49*, 2587−2595.
(2) Dick, J. E.; Hilterbrand, A. T.; Boika, A.; Upton, J. W.; Bard, A. J. *Proc. Natl. Acad. Sci. U. S. A.* **2015**, *112*, 5303−5308.
(3) Dick, J. E.; Hilterbrand, A. T.; Strawsine, L. M.; Upton, J. W.; Bard, A. J. *Proc. Natl. Acad. Sci. U. S. A.* **2016**, *113*, 6403−6408.
(4) Bard, A. J.; Zhou, H. J.; Kwon, S. J. *Isr. J. Chem.* **2010**, *50*, 267−276.
(5) Dick, J. E.; Renault, C.; Bard, A. J. *J. Am. Chem. Soc.* **2015**, *137*, 8376−8379.
(6) Dick, J. E.; Renault, C.; Kim, B. K.; Bard, A. J. *Angew. Chem., Int. Ed.* **2014**, *53*, 11859−11862.
(7) Kim, B.-K.; Boika, A.; Kim, J.; Dick, J. E.; Bard, A. J. *J. Am. Chem. Soc.* **2014**, *136*, 4849−4852.
(8) Kwon, S. J.; Zhou, H. J.; Fan, F. R. F.; Vorobyev, V.; Zhang, B.; Bard, A. J. *Phys. Chem. Chem. Phys.* **2011**, *13*, 5394−5402.
(9) Lebegue, E.; Anderson, C. M.; Dick, J. E.; Webb, L. J.; Bard, A. J. *Langmuir* **2015**, *31*, 11734−11739.
(10) Zhou, Y. G.; Rees, N. V.; Compton, R. G. *Angew. Chem., Int. Ed.* **2011**, *50*, 4219−4221.
(11) Haddou, B.; Rees, N. V.; Compton, R. G. *Phys. Chem. Chem. Phys.* **2012**, *14*, 13612−13617.
(12) Xiao, X.; Bard, A. J. *J. Am. Chem. Soc.* **2007**, *129*, 9610−9612.
(13) Dick, J. E.; Bard, A. J. *J. Am. Chem. Soc.* **2015**, *137*, 13752−13755.
(14) Dick, J. E.; Bard, A. J. *J. Am. Chem. Soc.* **2016**, *138*, 8446−8452.
(15) Yu, Y.; Noël, J.-M.; Mirkin, M. V.; Gao, Y.; Mashtalir, O.; Friedman, G.; Gogotsi, Y. *Anal. Chem.* **2014**, *86*, 3365−3372.

DOI: 10.1021/acs.analchem.7b03355
Anal. Chem. 2018, 90, 1142−1146